Vanadyl(IV) Phosphonates, VOC$_n$H$_{2n+1}$PO$_3$·xH$_2$O (n = 0–4, x = 1 or 1.5), as Precursors of Vanadyl(IV) Pyrophosphate, (VO)$_2$P$_2$O$_7$

V. V. Guliants, J. B. Benziger,* and S. Sundaresan

Princeton Materials Institute, Princeton University, Princeton, New Jersey 08544

I. E. Wachs and J.-M. Jehng

Zettlemoyer Center for Surface Studies, Lehigh University, Bethlehem, Pennsylvania 18015

Vanadyl(IV) phosphonates with the formula VOC$_n$H$_{2n+1}$PO$_3$·xH$_2$O (n = 0–4, x = 1 or 1.5) have been synthesized in organic medium by reaction of V$_2$O$_5$ with the corresponding phosphonic acid. The low-temperature magnetic susceptibility of vanadyl(IV) phosphite (n = 0) and n-butylphosphonate (n = 4) was indicative of antiferromagnetically exchange-coupled V$_2$O$_9$ vanadyl dimers similar to previously reported results for n = 1–3 phosphonates and vanadyl(IV) hydrogen phosphate hemihydrate (VOHPO$_4$·0.5H$_2$O). Raman spectroscopy of vanadyl(IV) phosphonates (n = 0–4) also suggested the similar local crystalline order in these solids. The close structural relationship between these phosphonates and VOHPO$_4$·0.5H$_2$O is further substantiated by the thermal transformation of the former phases in the presence of oxygen into vanadyl(IV) pyrophosphate. Kinetic measurements of the n-butane selective oxidation to maleic anhydride demonstrated that vanadyl methylphosphonate (n = 1) and phoshite (n = 0) produced vanadyl pyrophosphate catalysts with comparable (the methylphosphonate) and even superior performance (vanadyl phosphite) compared to the conventional unpromoted vanadium–phosphorus–oxide (VPO) catalyst.

Introduction

Vanadium–phosphorus–oxide (VPO) system is a well-known commercial catalyst for partial oxidation of C$_4$ hydrocarbons to maleic anhydride.[1] Vanadyl(IV) pyrophosphate is claimed to be the active phase of commercial catalysts;[2] it is produced by the pyrolitic transformation of the precursor phase, vanadyl(IV) hydrogen phosphate hemihydrate. The structural similarity between vanadyl pyrophosphate and its pyrolitic precursor is manifested in the presence of vanadyl dimers in both structures connected through corners by P$_2$O$_7$ or HPO$_4$ groups, respectively. The catalytic properties of vanadyl pyrophosphate have been associated with the V$_2$O$_8$ dimers on its (200) plane.

A variety of VPO phases have been synthesized based on the accessibility of different oxidation states of vanadium.[3] P(III) and P(IV) reduced oxyacids have been isolated,[4] but little is known about potential catalytic applications of corresponding V(IV)/P(III) or P(IV) compounds. Johnson et al. synthesized a number of the layered V(IV) organophosphonates[5–13] with the general formula VORAO$_3$·S, where R is an organic group, A is P(III) or As(III), and S is a solvent molecule.[6] Magnetic susceptibility data indicated that vanadyl methyl-, ethyl-, and propylphosphonates exhibited the same in-layer structure observed in layered vanadyl(IV) hydrogen phosphate hemihydrate, VOHPO$_4$·0.5H$_2$O.[14]

We have recently reported the synthesis and characterization of vanadyl(IV) phosphite, the n = 0 phase, which possesses the same structure of the vanadyl(IV) alkylphosphonates (n = 1–3).[15] Vanadyl(IV) phosphite transformed into vanadyl(IV) pyrophosphate at 523 K, suggesting that it may represent a new precursor to active VPO catalysts.

® Abstract published in *Advance ACS Abstracts,* July 1, 1995.

(1) Centi, G.; Trifirò, F.; Ebner, J. R.; Franchetti, V. M. *Chem. Rev.* **1988,** *88,* 55.

(2) Centi, G. *Catal. Today* **1993,** *16,* 5.

(3) (a) Wang, S. L.; Kang, H. Y.; Chen, C. Y.; Lii, K. H. *Inorg. Chem.* **1991,** *30,* 3496. (b) Huan, G.; Johnson, J. W.; Jacobson, A. J.; Corcoran, E. W., Jr.; Goshorn, D. P. *J. Solid State Chem.* **1991,** *93,* 514. (c) Lii, K. H.; Mao, L. F. *J. Solid State Chem.* **1992,** *96,* 436. (d) Lii, K. H.; Chueh, B. R.; Kang, H. Y.; Wang, S. L. *J. Solid State Chem.* **1992,** *99,* 72. (e) Gopalakrishnan, J.; Rangan, K. K. *Chem. Mater.* **1992,** *4,* 745. (f) Matsubayashi, G.; Nakajima, H. *Chem. Lett.* **1993,** 31. (g) Haushalter, R. C.; Wang, Z.; Thompson, M. E.; Zubieta, J.; O'Connor, C. J. *Inorg. Chem.* **1993,** *32,* 3966. (h) Haushalter, R. C.; Wang, Z.; Thompson, M. E.; Zubieta, J. *Inorg. Chem.* **1993,** *32,* 3700. (i) Soghomonian, V.; Chen, Q.; Haushalter, R. C.; Zubieta, J.; O'Connor, C. J. *Science* **1993,** *259,* 1596.

(4) (a) Ohashi, S. In *Topics in Phosphorus Chemistry;* Grayson, M., Griffith, E. J., Eds.; Interscience Publishers: New York, 1964; Vol. 1, pp 152–187. (b) Corbridge, D. E. C. *Phosphorus: An Outline of Its Chemistry, Bochemistry and Technology,* 4th ed.; Elsevier: Amsterdam, 1990, and references therein.

(5) Johnson, J. W.; Jacobson, A. J.; Brody, J. F.; Lewandowski, J. T. *Inorg. Chem.* **1984,** *23,* 3842.

(6) Johnson, J. W.; Jacobson, A. J. EP 134157 A2, 1985.

(7) Jacobson, A. J.; Johnson, J. W. *Mater. Sci. Monogr., 28A (React. Solids, Pt. A)* **1985,** 469.

(8) Johnson, J. W.; Jacobson, A. J.; Butler, W. M.; Rosenthal, S. E.; Brody, J. F.; Lewandowski, J. T. *J. Am. Chem. Soc.* **1989,** *111,* 381.

(9) Huan, G.; Jacobson, A. J.; Johnson, J. W.; Concoran, E. W., Jr. *Chem. Mater.* **1990,** *2,* 91.

(10) Johnson, J. W.; Brody, J. F.; Alexander, R. M. *Chem. Mater.* **1990,** *2,* 198.

(11) Huan, G.; Johnson, J. W.; Jacobson, A. J.; Merola, J. S. *J. Solid State Chem.* **1990,** *89,* 220.

(12) Huan, G.; Jacobson, A. J.; Day, V. W. *Angew. Chem., Int. Ed. Engl.* **1991,** *30,* 422.

(13) Huan, G.; Jacobson, A. J.; Johnson, J. W.; Goshorn, D. P. *Chem. Mater.* **1992,** *4,* 661.

(14) Johnson, J. W.; Johnston, D. C.; Jacobson, A. J.; Brody, J. F. *J. Am. Chem. Soc.* **1984,** *106,* 8123.

(15) Guliants, V. V.; Benziger, J. B.; Sundaresan, S. *Chem. Mater.,* in press.

Table 1. Interlayer Spacings and Elemental Compositions of $VOC_nH_{2n+1}PO_3 \cdot xH_2O$ ($n = 0-4$) Phases

n	0	1	2	3	4
d, Å	7.28	8.32	9.73	11.19	12.79
d, Å[17]		8.304	9.70	11.10	15.48
V, %	28.26	27.56	23.78	23.16	21.77
P, %	15.93	17.30	15.33	14.52	12.65
C, %	0.77	6.96	12.51	16.69	21.83
H, %	2.76	3.06	3.78	4.47	5.21
P/V	0.93	1.03	1.06	1.03	0.96
C/P	0.12	1.04	2.11	2.97	4.46
x (TGA)	1.75	1.65	1.53	1.51	1.06

We report here the synthesis and characterization of a new layered vanadyl(IV) *n*-butylphosphonate and other short-chain alkylphosphonates (R = H, Me, Et, and Pr; S = 1.5- or 1H$_2$O). The present work demonstrates that short alkyl chain vanadyl phosphonates represent a new class of precursors to vanadyl pyrophosphate catalysts. Our results show that the vanadyl phosphite-derived catalysts displayed performance superior to that obtained from conventional unpromoted VPO catalysts obtained from VOHPO$_4$·0.5H$_2$O.

Experimental Section

Synthesis. Vanadium pentoxide (Aldrich) was refluxed in anhydrous ethanol (Aldrich) for 16 h. Phosphonic acid (Aldrich) dissolved in anhydrous ethanol was then added to achieve a P/V ratio of 1.0−1.3. The reaction mixture was refluxed for another 20 h during which time the color of the suspended solids changed to light blue. The light blue solids were separated by filtration, washed with ethanol and acetone and dried in air. Elemental analysis (Table 1) was consistent the formula

$$VOC_nH_{2n+1}PO_3 \cdot xH_2O \quad (n = 0-4, x = 1 \text{ or } 1.5)$$
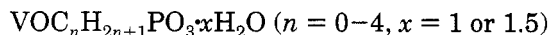
Characterization. Powder X-ray diffraction patterns were recorded with Scintag/USA DMS 2000 diffractometer using a Cu Kα radiation. The Raman spectra were obtained with a Spectra-Physics Ar$^+$ laser (Model 171) by using ca. 25−50 mW of the 514.5-nm line for excitation. About 100−200 mg of the powdered solid was pressed into a thin wafer about 1 mm thick with KBr backing for support. The sample was then mounted onto a spinning sample holder and rotated at ca. 2000 rpm to avoid local heating effects. A 90° collection geometry was employed to collect the scattered light. The powdered vanadyl phosphonates were pressed into a pellet (7 mm diameter, 1 mm thick) under 3000 psi for magnetic susceptibility measurements. The XRD pattern of the pellet was identical with the one of the powdered solid. Magnetic susceptibility data were collected on SQUID magnetometer (Quantum Design, MPMS system) with the pellet C_2 axis parallel to magnetic field $H = 6.35$ kG. Magnetization (M) isotherms collected at 20, 100, and 295 K were linear in the applied magnetic fields (H) of 2−8 kG, and the saturation magnetization arising from the ferromagnetic impurities was found to be negligibly small. Thermogravimetric analysis of the phosphonates was performed in air on a Perkin-Elmer TGS-2 thermal analyzer. BET surface areas were measured by nitrogen adsorption on Quantachrome Quantasorb system. Elemental microanalysis of the solids for V, P, C, and H was performed by Robertson Microlit Laboratories, Madison, NJ.

Kinetic Tests. Oxidation of *n*-butane was carried out using ca. 1 g of vanadyl(IV) phosphonate sieved to 35−65 mesh. The phosphonate was placed into a U-tube Pyrex glass reactor inside an aluminum split block and activated at 708 K in 1.2% *n*-butane in dry air at a space velocity of 400 h^{-1} for 7 days. This activation produced the most selective catalysts from VOHPO$_4$·0.5H$_2$O precursors.[16] All experiments were carried out in a once-through integral mode. CP grade *n*-butane from
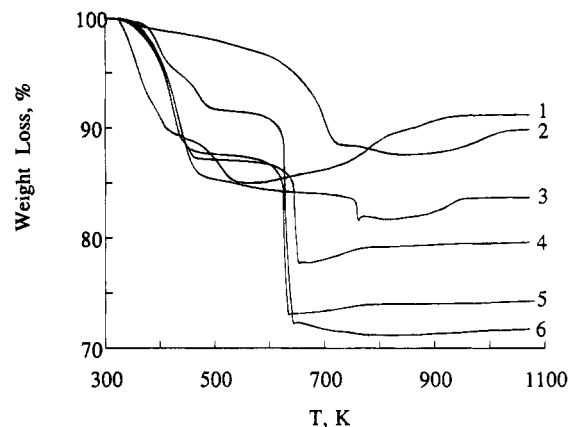
Figure 1. TGA curves of vanadyl(IV) phosphonates in air. Heating rate 10 K/min. (1) $n = 0$, (2) VOHPO$_4$·0.5H$_2$O, (3) $n = 1$, (4) $n = 2$, (5) $n = 3$, (6) $n = 4$.

Matheson and dry air were metered separately using Brooks Model 52-36A1V Series mass flow controllers with Model 5876 two-channel power supply box and mixed in desired proportions. Only a small fraction of the total flow was metered to the reactor, the rest being vented.

The effluent stream was analyzed by on-line gas chromatography. The lines from the reactor to gas chromatographs were kept at 420 K to prevent condensation of maleic anhydride. A side stream ran from the heated effluent line to a HP 5790A Series gas chromatograph where partial oxidation products (mainly MA and traces of acetic and acrylic acids) were separated on a 2 m long Porapak QS column. The bulk of the reactor effluent was directed through a water bubbler that stripped the partial oxidation products. The effluent samples from a sample loop were then injected into two GC columns in series : a 5 m long 30% bis-2-ethoxyethyl sebacate column to separate CO$_2$ and butane, and a 4 m long molecular sieve 13X one to separate O$_2$, N$_2$, and CO.

Separate samples of vanadyl phosphonates were activated in a Lindberg tubular oven at 623 or 723 K (see below) in 15 cm^3/min 1.2% *n*-butane in air for 6 h in order to study their thermal transformation.

Results

The elemental analysis of the vanadyl phosphonates is listed in Table 1. The V/P/C ratios are consistent with the composition of vanadyl phosphonate (VOC_nH_{2n+1}-PO$_3 \cdot xH_2O$, $n = 0-4$). Thermal gravimetric analysis was used to further clarify the composition. TGA curves of the $n = 0-4$ vanadyl alkylphosphonates and VOH-PO$_4$·0.5H$_2$O are shown in Figure 1. The $n = 1-4$ phosphonates show an initial weight loss between 330−500 K, which we attribute to the loss of structural and intercalated water molecules. In the case of vanadyl phosphite ($n = 0$), the water content (Table 1) was determined from the total weight loss by TGA in air at 1073 K according to the stoichiometric oxidation of VOHPO$_3 \cdot xH_2O$ into VOPO$_4$.[15] For $n = 0-3$ the water content is 1.5H$_2$O per unit formula, with the excess water probably resulting from intercalated or adsorbed water. The TGA for the butylphosphonate was distinctly different. There was less weight loss for the water and the stoichiometry was 1.0H$_2$O per unit formula.

A second sharp weight loss occurred at 750 K for the methylphosphonate and 650 K for ethyl-, propyl-, and butylphosphonates that corresponds to the combustion

(16) J. S. Buchanan, J. S.; Sundaresan, S. *Appl. Catal.* **1986**, *26*, 211.

Precursors of Vanadyl(IV) Pyrophosphate

Chem. Mater., Vol. 7, No. 8, 1995 1495
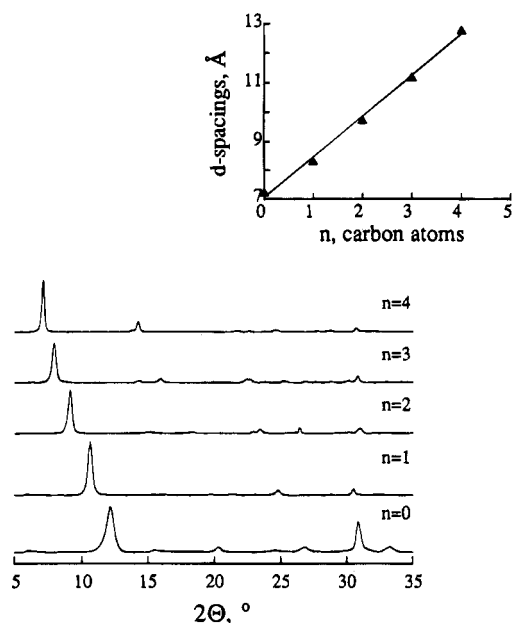
Figure 2. XRD patterns of vanadyl(IV) *n*-alkylphosphonates ($n = 0-4$). Inset: layer spacings of the type B vanadyl(IV) phosphonates ($n = 0-4$) as a function of carbon number (n).

Figure 3. Magnetic susceptibility data for (A) vanadyl(IV) phosphite and (B) vanadyl(IV) butylphosphonate. Dotted lines represent fits to the Bleaney–Bowers expression (please see the text).

of the alkyl group and transformation to vanadyl pyrophosphate (vide infra). In the case of vanadyl phosphite, the combined weight loss from 303 to 550 K corresponded to dehydration and oxidation of the phosphite groups completing the transformation of the phosphite to vanadyl pyrophosphate.[15] At temperatures above 700 K all the phosphonates (or 600 K in the case of vanadyl phosphite) showed a weight gain corresponding to oxidation of vanadyl pyrophosphate to vanadyl(V) orthophosphate, $VOPO_4$.[15]

X-ray diffraction, magnetic susceptibility, and Raman spectroscopy have been used to elucidate the structure of the vanadyl phosphonates. With the rare exceptions, e.g., vanadyl(IV) phenyl phosphonate,[9] the crystalline quality of these compounds has not been sufficient to determine the structure by XRD methods. Interlayer spacings in the *n*-alkylphosphonates as a function of the alkyl chain length were determined by XRD.[17] The XRD patterns for the series $VOC_nH_{2n+1}PO_3 \cdot xH_2O$ ($n = 0-4$, $x = 1$ or 1.5) synthesized in this work are shown in Figure 2, and the interlayer spacings, d, vs number of carbon atoms, n, are given by $d = 7.13 + 1.33n$ (Å) (see inset in Figure 2).

Magnetic susceptibility has been used as a check to distinguish the two major V–P–O connectivities occurring in vanadyl phosphonates. The ability of the system to crystallize in either corner-sharing (type A) or the vanadyl dimer-type structure (type B) is determined by the packing constraints of the organo group attached to phosphorus on the vanadyl phosphonate layer.[5] Vanadyl phenylphosphonate mono- or dihydrate are examples of the type A solids. In such materials the V=O···V=O chains or VO_5H_2O octahedra are connected through corners by the RPO_3 tetrahedra forming a layered solid with the alkyl groups pointed towards the interlayer space. The magnetic susceptibility for such V–P–O connectivity either shows no deviation from the Curie–Weiss behavior in the entire 4–300 K temperature range.[10]
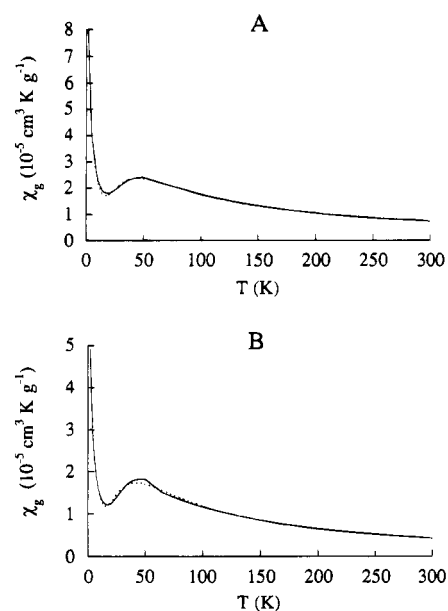
Johnson et al.[17] proposed that vanadyl phosphonates with the small alkyl groups (n = 1–3) belonged to type B solids. In these solids the magnetic susceptibility as a function of temperature displays a maximum at $T <$ 100 K characteristic of antiferromagnetically exchange-coupled dimers.[17] The magnetic susceptibility as a function of temperature for the new members of the phosphonate family, vanadyl phosphite ($n = 0$)[15] and *n*-butylphosphonate ($n = 4$) is shown in Figure 3A and B. The data in Figure 3 have been analyzed using Bleaney–Bowers expression for an isolated dimer model containing two $S = \frac{1}{2}$ cations with isotropic g tensor:[13]

$$\chi = \chi_0 + C_i/(T - \Theta) + 4C_d/(T(3 + \exp(-2J/k_BT)))$$

where χ_0 is the temperature independent contribution; C_d, the Curie constant associated with the vanadyl dimers; C_i and Θ, the constants associated with the magnetic impurities; and J, the coupling constant within the vanadyl pairs. The analogous behavior of magnetic susceptibility at temperatures below 100 K was observed in case of vanadyl hydrogen phosphate hemihydrate ($VOHPO_4 \cdot 0.5H_2O$) where direct correlation with the presence of the face-sharing $V_2O_8(H_2O)$ dimers in the crystal structure was found.[14] The parameters of the least square fits to the magnetic susceptibility data for the type B solids including the new phosphonates ($n = 0$ and 4) and $VOHPO_4 \cdot 0.5H_2O$ are given in Table 2.

Raman spectroscopy is sensitive to the local bonding structure in metal phosphonates.[18] The Raman spectra of the type B solids including the new $n = 0$ and 4 vanadyl phosphonates and $VOHPO_4 \cdot 0.5H_2O$ are shown in Figure 4. The peak positions in the spectra of the $n = 0-4$ phosphonates are given in Table 3. The spectra of the type B alkylphosphonates and $VOHPO_4 \cdot 0.5H_2O$

(17) Huan, G.; Johnson, J. W.; Brody, J. F.; Goshorn, D. P. *Mater. Chem. Phys.* **1993**, *35*, 199.

(18) Bujoli, B.; Palvadeau, P.; Queignec, M. *Eur. J. Solid State Inorg. Chem.* **1992**, *29*, 141.

Table 2. Magnetic Susceptibility Data for
VOC$_n$H$_{2n+1}$PO$_3\cdot x$H$_2$O (n = 0–4) and VOHPO$_4\cdot$0.5H$_2$O^a

n	C_d, 10^{-3} cm^3 K g^{-1}	$2J/k_B$, K	C_i, 10^{-5} cm^3 K g^{-1}	θ, deg	χ_0, 10^{-7} cm^3 K g^{-1}	μ_{eff}, μ_B
VHP^b	2.12	−88	4.0	0	−3	1.72
0	1.90	−84.5	23.6	−1.0°	9.87	1.73
1^c	2.00	−43.8	5.26	−5.3°	−4.44	1.75
2^c	1.89	−51.6	2.82	0	−9.60	1.75
3^c	1.75	−52.0	2.40	0	−7.86	1.74
4	1.38	−78.2	16.9	−1.4°	−5.16	1.69

^{a} VHP = VOHPO$_4\cdot$0.5H$_2$O. ^{b} Data from ref 14. ^{c} Data from ref 17.
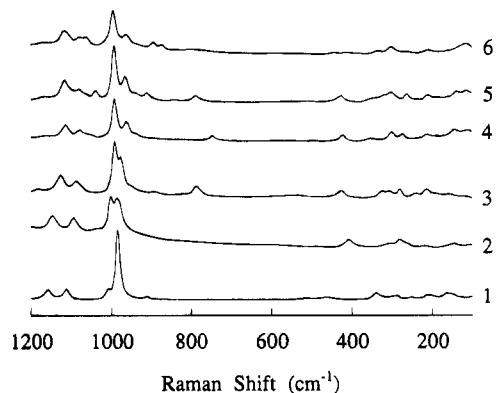
Figure 4. Raman spectra of (1) VOHPO$_4\cdot$0.5H$_2$O and VOC$_n$-H$_{2n+1}$PO$_3\cdot x$H$_2$O: (2) n = 0, (3) n = 1, (4) n = 2, (5) n = 3, and (6) n = 4.
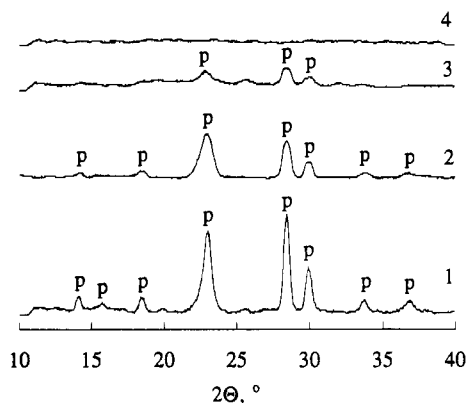

Figure 5. XRD patterns of vanadyl pyrophosphate samples produced after the thermal treatment of VOC$_n$H$_{2n+1}$PO$_3\cdot$ xH$_2$O: (1) n = 0, (2) n = 1, (3) n = 2, and (4) n = 3. The n = 4 sample is amorphous. p = (VO)$_2$P$_2$O$_7$.

exhibit a number of common features, including P–O stretches between 1000–1200 cm^{-1}, V=O stretch at 990–1010 cm^{-1}, coupled V–O and P–O bending modes between 150 and 600 cm^{-1}. The phosphonates also show distinct P–C stretching modes at ca. 740–790 cm^{-1} and PO$_3$ bending modes between 420 and 550 cm^{-1}.

X-ray diffraction patterns and Raman spectra of the vanadyl(IV) phosphonates were taken after calcining the samples in 1.2% n-butane in air for 6 h at 623 (n = 0, 2, 3, 4) and 723 K (n = 1). Powder XRD patterns are shown in Figure 5. The only crystalline phase detected by XRD was vanadyl pyrophosphate. Crystallinity (based on the fwhm of the XRD peaks) was greater for vanadyl phosphite (n = 0) and diminished as the alkyl chain length in the vanadyl phosphonate precursor increased, such that the butylphosphonate yielded a completely XRD amorphous sample.
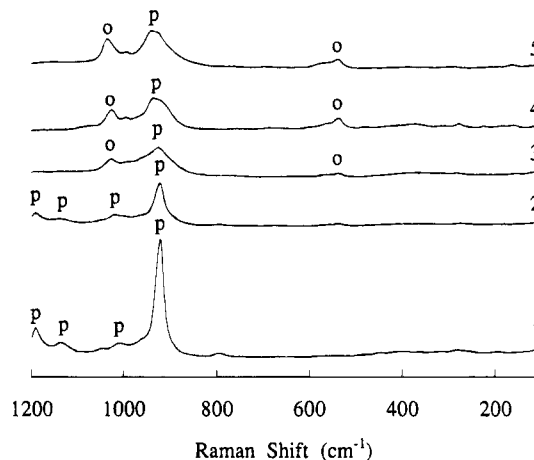
Figure 6. Raman spectra of vanadyl pyrophosphate samples produced after the thermal treatment of VOC$_n$H$_{2n+1}$PO$_3\cdot$ xH$_2$O: (1) n = 0, (2) n = 1, (3) n = 2, (4) n = 3 and (5) n = 4. p = (VO)$_2$P$_2$O$_7$, o = α_I- or α_{II}-VOPO$_4$.
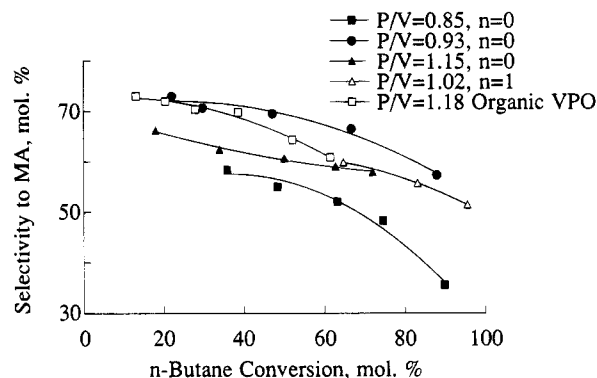
Figure 7. Selectivity to maleic anhydride vs n-butane conversion at 654 K in 1.2% n-butane–air for VPO catalysts produced from VOC$_n$H$_{2n+1}$PO$_3\cdot x$H$_2$O phases with n = 0 (phosphite) and n = 1 (methylphosphonate) and from the VOHPO$_4\cdot$0.5H$_2$O (organic) precursor.

Raman spectra for the thermally transformed phosphonates are shown in Figure 6. The Raman spectra also show diminishing intensity of the strong PO$_3$ stretching feature of vanadyl pyrophosphate at 921–925 cm^{-1} with the alkyl chain length. The Raman spectrum of the vanadyl butylphosphonate sample which is amorphous in XRD (Figure 6) shows a broad band at ca. 950–920 cm^{-1} indicative of disordered vanadyl pyrophosphate phase. For the n = 2–4 vanadyl alkylphosphonates the calcined samples also show the presence of VOPO$_4\cdot$2H$_2$O as evidenced by Raman peaks at 530, 998, and 1035 cm^{-1}.[19]

The performance of VPO catalysts derived from vanadyl phosphite and vanadyl methylphosphonate precursors for the partial oxidation of n-butane to maleic anhydride were evaluated. Three samples of vanadyl phosphite with different bulk phosphorus-to-vanadium (P/V) ratios and vanadyl methylphosphonate with P/V = 1.02 were activated in the flow reactor. The dependence of selectivity to maleic anhydride on n-butane conversion shown in Figure 7. For comparison, the selectivity-conversion relationship for a sample of conventional unpromoted catalyst[20] prepared and tested in our laboratory is also shown. Vanadyl methylphospho-

(19) Guliants, V. V.; Benziger, J. B.; Sundaresan, S.; Wachs, I. E.; Jehng, J.-M.; Roberts, J. E. *J. Catal.*, in press.

Table 3. Raman Peaks of VOC$_n$H$_{2n+1}$PO$_3 \cdot x$H$_2$O Phases (n = 0–4) at Room Temperature^a

n = 0	1094 vW, 1146 M, 1093 M, 1042 W, 1001 vS, 985 vS, 407 M, 306 W, 282 M, 222 W, 147 W
n = 1	1182W, 1125 M, 1087 M, 991 vS, 976 vS, 891 W, 787 M, 426 M, 324 W, 308 W, 281 W, 241 W, 214 M, 159 vW
n = 2	1164 vW, 1113 M, 1079 W, 992 vS, 962 M, 746 W, 422 M, 355 W, 302 M, 273 M, 213 W, 143 M, 109 W
n = 3	1168 vW, 1115 M, 1079 W, 1038 W, 993 vS, 965 M, 939, W sh, 910 W, 788 W, 426 M, 303 W br, 263 W, 211 W, 139 W, 114 W
n = 4	1168 vW, 1116 M, 1077 W, 1063 W, 994 vS, 963 M, 894 W, 874 W, 798 vW br, 442 vW, 411 vW, 302 W, 210 W, 112 W

^{a} Labels: vS = very strong, S = strong, M = medium, W = weak, vW = very weak, br = broad, sh = shoulder.

nate produced a VPO catalyst of similar performance, while the P/V = 0.93 vanadyl phosphite sample exhibited considerably higher selectivities than the organic catalyst at n-butane conversions above 40% (Figure 7). Under reaction conditions the BET surface area of the methylphosphonate sample increased from 19 to 23.3 m^2/g, the surface area of P/V = 0.85 and 1.13 vanadyl phosphite samples increased from 20.0 and 20.7 m^2/g to 40.9 and 43.4 m^2/g, respectively, while the surface area of the most selective catalyst with P/V = 0.93 increased from 12.9 to 37.7 m^2/g. These values are high for the unpromoted VPO system where surface areas do not generally exceed 20 m^2/g. The BET surface areas of the unpromoted organic catalyst employed was found to be 11.3 m^2/g. Such high surface areas observed in the vanadium phosphite system are crucial for obtaining both selective and active VPO catalysts.

Discussion

Vanadyl(IV) alkylphosphonates (n = 0–4) with the type B structure containing V$_2$O$_8$ dimers represent a new class of precursors to vanadyl pyrophosphate catalysts for the selective oxidation of n-butane. This is the first report of the use of these compounds as catalytic precursors, and the impressive results obtained suggest that they may be the source of new improved VPO catalysts.
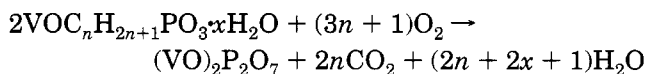
The use of the phosphonate precursors was motivated by the similarity in structure between vanadyl phosphonates and the conventional vanadyl hydrogen phosphate hemihydrate precursor. The transformation of VOHPO$_4 \cdot$0.5H$_2$O into a selective vanadyl pyrophosphate catalyst relies on the existence of vanadyl dimers in both structures. Johnson et al. showed that magnetic susceptibility data of the n = 1–3 vanadyl n-alkylphosphonates indicated that these compounds also contained vanadyl dimers.[17] Our work reported here and in a previous paper[15] extends the range of groups to n = 0 (H atom) and n = 4 (n-butyl group). Johnson et al.[17] suggested that vanadyl(IV) n-butylphosphonate contained only isolated vanadyl octahedra as opposed to vanadyl dimers. Our data do suggest a change in structure for the butylphosphonate as the water content was less for n = 4 than the n = 0–3 compounds. However, the magnetic susceptibility and interlayer spacings by XRD suggest that vanadyl butylphosphonate is still a type B structure containing the V$_2$O$_8$ dimers. The number of magnetic defects in the butyl phosphonate was greater than for the n = 1–3 compounds, as evidenced by the larger value of C_i in the Bleaney–Bowers fit to the data (Table 2). The defects may be associated with decreased stability of the vanadyl dimers in the butyl phosphonate. Vanadyl phosphite also shows a greater content of magnetic

impurities, which suggests that hydrogen may be too small to force the ordering of the vanadyl dimers.

We have found that the solvent used during the reaction of the phosphonic acid and vanadium pentoxide can alter the structure of vanadyl phosphonate formed. Vanadyl phosphite containing vanadyl dimers was only formed when small alcohols, e.g., ethanol or propanol, were used, and a structure containing isolated vanadyl octahedra resulted when ethanol was substituted with benzyl alcohol.[15] It seems likely that our synthesis procedure and that of Johnson and co-workers varied enough to result in two different structures formed. The data in Figure 2 show an excellent linear fit to the interlayer spacing with the alkyl chain length for n = 0 to n = 4, indicating that all the phosphonates have a common layer structure despite the fact that the n = 0–3 phosphonates and the butylphosphonate have 1.5H$_2$O and 1H$_2$O per unit formula, respectively (Table 1 here and ref 17). The data of Johnson et al. showed a discontinuity in the interlayer spacings between n = 1–3 and n = 4 phases (Figures 2 and 3 in ref 17).

The degree of the layer stacking order in the vanadyl n-alkylphosphonates is also dependent on the alkyl chain length. The peaks in the XRD patterns (Figure 2) corresponding to interlayer spacing become sharper with longer chain reflecting increased layer stacking order due to van der Waals interaction between the alkyl chains. The Raman P–O and P–C stretches shown in Figure 4 become weaker and more diffuse with increasing size of n-alkyl indicative of both the decreasing content of these chromophores and poor crystalline order.

Vanadyl(IV) phosphonates (n = 0–4) were converted to vanadyl pyrophosphate upon heating in oxygen-containing atmosphere. This result gives further support to the hypothesis that the vanadyl dimers are the key to creating the structure of vanadyl pyrophosphate.[15] The TGA results shown in Figure 1 compare the weight losses for vanadyl phosphonates to VOHPO$_4 \cdot$0.5H$_2$O. Except for the methylphosphonate, vanadyl phosphonates convert to vanadyl pyrophosphate at lower temperatures than VOHPO$_4 \cdot$0.5H$_2$O. Furthermore, the structural and intercalated water is also removed at lower temperatures than in the case of VOHPO$_4 \cdot$0.5H$_2$O. The structural and intercalated water in the phosphonates is involved in weaker interlayer bonding than the structural water in VOHPO$_4 \cdot$0.5H$_2$O. These weak interlayer interactions are key to the ease of removing the water and oxidizing the alkyl groups on the phosphonate layer. The alkyl groups are oxidized converting the P(III) to P(V). The overall transformation of vanadyl(IV) phosphonates is described by

$$2\text{VOC}_n\text{H}_{2n+1}\text{PO}_3 \cdot x\text{H}_2\text{O} + (3n + 1)\text{O}_2 \rightarrow$$
$$(\text{VO})_2\text{P}_2\text{O}_7 + 2n\text{CO}_2 + (2n + 2x + 1)\text{H}_2\text{O}$$

In vanadyl(IV) phosphite the loss of the intercalated (1H$_2$O) and structural (0.5H$_2$O) water at 273–550 K

(20) Milberger, E . C.; Bremer, N. J.; Dria, D. E. U. S. Patent 4,333,853 **1982**.

overlaps the process of P—H group oxidation into P—OH accompanied by the loss of water ($0.5H_2O$). A weight gain ($0.5O_2$ per unit formula of $VOHPO_3 \cdot 1.5H_2O$) expected in such oxidation is overshadowed by the loss of water ($-2H_2O$), and no weight gain is observed until oxidation of $(VO)_2P_2O_7$ becomes noticeable above 600 K. Vanadyl(IV) phosphite is rapidly converted into vanadyl pyrophosphate below 550 K, at temperatures nearly 200 K lower than required for $VOHPO_4 \cdot 0.5H_2O$. This low-temperature conversion of vanadyl phosphite to vanadyl pyrophosphate is crucial for excellent catalytic performance of this catalyst. Vanadyl(V) orthophosphates formed in the presence of oxygen at high temperature are not selective for n-butane oxidation.[19] Since vanadyl phosphite yields vanadyl pyrophosphate at low temperature, the overoxidation to V(V) phases is avoided producing a better catalyst. Vanadyl(V) orthophosphate phases were observed after transformation of the n-alkylphosphonates, the amount of the orthophosphate phases increasing with the alkyl chain length. We suggest that the $VOPO_4$ phases arise from local temperature excursions resulting from the exothermic combustion of the alkyl groups.

The last advantage of the vanadyl phosphite precursor to vanadyl pyrophosphate is that it yields catalysts possessing greater surface area than the conventional unpromoted VPO catalysts. This probably results from a smaller crystallite size. The lower activation temperature for vanadyl phosphite reduces sintering of the crystallites.

Conclusions

New vanadyl phosphonates ($n = 0$ and 4) display antiferromagnetic exchange interactions at low temper-

atures associated with presence of face-sharing vanadyl dimers similar to $VOHPO_4 \cdot 0.5H_2O$ and the $n = 1-3$ phosphonates.[17] Raman spectroscopy, the correlation of layer spacings vs carbon number in the phosphonate alkyl chain, magnetic susceptibility data and thermal transformations to vanadyl pyrophosphate provided evidence of the close structural relationship between $VOHPO_4 \cdot 0.5H_2O$ and vanadyl(IV) phosphonates ($n = 0-4$) based on the presence of face-sharing vanadyl dimers.

Vanadyl phosphonates ($n = 0$ and 1) have been found to yield highly active and selective vanadyl pyrophosphate catalysts for partial oxidation of n-butane to maleic anhydride. The VPO catalyst (P/V=0.93) produced from vanadyl phosphite had higher surface areas and higher selectivities to maleic anhydride at higher n-butane conversions than conventional organic catalyst.

Preparation of well-crystallized vanadyl(IV) phosphonates ($n = 0-4$) for their structure solution, with the exception of vanadyl methylphosphonate, still remains a challenge. Synthetic efforts in this direction are currently under way.

CM950008L